PHY Abstraction Techniques for IEEE 802.11p and LTE-V2V: Applications and Analysis

Waqar Anwar, Kedar Kulkarni, Thomas R. Augustin, Norman Franchi and Gerhard Fettweis
Vodafone Chair Mobile Communications Systems, Technische Universität Dresden, Germany
{waqar.anwar, kedar.kulkarni, thomas.augustin, norman.franchi, gerhard.fettweis}@tu-dresden.de

***Abstract*—IEEE 802.11p and LTE-V2V are wireless standards of interest to enable connected and autonomous driving. To evaluate and compare the performance of these technologies under different channel conditions and reliability requirements, system level evaluations are required. For this purpose, we first present physical layer abstraction (PLA) techniques for IEEE 802.11p and LTE-V2V and then compare their performance using system level simulations. Using the proposed PLA methods, we compare the considered technologies in terms of throughput, latency and reliability. The results show that expected throughput, latency and packet error rate achieved by the proposed PLA methods are close to the bound obtained through full PHY simulations.**

***Index Terms*—PHY abstraction, System-level simulation, Connected Vehicles, IEEE 802.11p, LTE-V2V, ITS**

I. Introduction

Vehicular communication aims to address multiple challenges in intelligent transportation systems (ITS) such as connected autonomous driving, cooperative maneuvering, smart navigation, and safety to vulnerable road users. Moreover, connected vehicles, pedestrians and infrastructures can collect and exchange information about the environment in real-time to perceive and avoid dangerous situations. To enable wireless access in vehicular environment (WAVE) and support V2X communications, dedicated short-range communication (DSRC) standards have been designed specifically focusing on vehicular safety applications. IEEE 802.11p was the first standardized technology enabling DSRC. LTE-V2V from 3GPP (3rd Generation Partnership Project) introduces advanced features for vehicle-to-vehicle (V2V) communication providing a suitable alternative to 802.11p [1]. In order to evaluate the performance of these technologies under varying channel and environmental conditions, reliability requirements and different scenarios, system-level evaluations are essential. PLA is an efficient tool to carry out these evaluations within affordable computational complexity. Specifically, it is used to model the link level performance such as throughput, latency and packet error rate (PER) solely in terms of received signal-to-noise-ratio (SNR). Therefore, the significance of system-level evaluations highly depend on the accuracy of the used PLA method.

In a wide-band multi-carrier system, each sub-carrier can undergo different fading conditions, hence the received SNR per sub-carrier can be different. In order to compute a single link quality metric (LQM), PLA maps the instantaneous SNRs of all sub-carriers to an effective SNR (ESNR). For orthogonal frequency division multiplexing (OFDM) based systems like 802.11p, received-bit-information-rate (RBIR) and exponential-effective-SNR-mapping (EESM) are the traditionally used PLA methods. In [2], [3] the accuracy of these methods have been verified under different fading conditions. However, these PLAs can not be used in single-carrier frequency division multiplexing (SC-FDM) based systems such as LTE-V2V. This is due to DFT-spread of symbols over all sub-carriers unlike OFDM where one symbol is transmitted on a single sub-carrier.

In this paper, we evaluate different PLA techniques for 802.11p and LTE-V2V. For 802.11p, we propose a new abstraction method, called *enhanced EESM* (eEESM), which outperforms existing PLA methods. In case of LTE-V2V, we propose to use average SNR of all sub-carriers as an effective SNR metric. Furthermore, we present a system-level simulation environment to evaluate performance of the considered PLAs in terms of estimated PER and throughput. The system level simulation results of different PLA methods are compared with the results achieved by physical layer simulations (PLS). In addition, PLAs are optimized according to the channel conditions and improvement in performance is shown. We also provide system-level comparison of both technologies based on the proposed PLA techniques.

II. Technologies Overview

In this section, we present an overview of technologies and highlight their physical layer aspects.

A. IEEE 802.11p

IEEE 802.11p is an amendment to IEEE 802.11 standard released in 2010 [4] for DSRC. In [5], [6], the performance of 802.11p has been evaluated in real world test scenarios with up to hundreds of vehicles. The physical (PHY) layer of 802.11p has eight possible combinations of MCS using convolution coding. An user equipment (UE) is able to adapt MCS according to the channel conditions. Depending on the selected MCS, raw

TABLE I
IEEE 802.11P: MCS + ACHIEVABLE DATA RATES & LATENCIES

MCS	Modulation	Code Rate	$\Gamma^{(11p)}$	$t_{tx}^{(11p)}$
0	BPSK	1/2	2.78 Mbps	0.576 ms
1	BPSK	3/4	4.00 Mbps	0.400ms
2	QPSK	1/2	5.13 Mbps	0.312 ms
3	QPSK	3/4	7.14 Mbps	0.224ms
4	16QAM	1/2	9.09 Mbps	0.176 ms
5	16QAM	3/4	11.76 Mbps	0.136 ms
6	64QAM	2/3	14.28 Mbps	0.112 ms
7	64QAM	3/4	15.38 Mbps	0.104 ms

P_b = 200 bytes and 10 MHz bandwidth

data rate varies between 3-27 Mbps. Similar to most 802.11 standards, 802.11p uses OFDM as modulation scheme, but with a lower channel bandwidth of just 10 MHz. The PHY frame consists of a fixed preamble (equal to 40 µs) and a variable amount of payload data (from upper layers). Table I provides an overview of the specified MCSs including data rates and transmission latencies that can be achieved in best case scenario for payload of 200 bytes.

B. LTE-V2V

In Release 12, 3GPP introduced device-to-device (D2D) functionalities to enable direct communications between two devices. Motivated by the huge interest from the vehicular community, 3GPP introduced specific features for vehicle-to-vehicle (V2V) communication in Release 14 [7]. Unlike 802.11p, LTE-V2V is based on SC-FDM. The symbol duration defined in LTE is 10 times larger than the symbol duration in 802.11p, which provides robustness against multi-path and reduces inter symbol interference (ISI). Furthermore, rather than using the complete bandwidth for transmission as in the case of 802.11p, it assigns a number of resource block (RBs) depending upon the payload size and selected MCS. However, the minimum transmission latency cannot be shorter than 1ms, which is the size of a sub-frame. Further, it specifies a continuous variation of MCS combinations with advanced coding schemes such as turbo codes [8], which results in higher reliability and transmission range compared to 802.11p. Table II provides an overview of MCS combinations including number of resource blocks and equivalent data rates for a payload of 200 bytes. The step by step procedure for calculating these values is explained in [1]. The transmission latency of all MCS is 1ms, except for MCS0, which is 2ms. The minimum SNR thresholds for used MCSs are given in Table II, which are obtained from Section III-F, Fig. 2 for a target reliability of PER $< 10^{-3}$.

III. PHYSICAL LAYER ABSTRACTION

In general, PLA maps SNRs on different sub-carriers to an effective SNR in order to compute a combined LQM. In this section, we introduce PLA methods, compare their performance for fading channel conditions, and investigate which abstraction model is most suitable for 802.11p and LTE-V2V.

TABLE II
LTE-V2V: MCS OPTIONS & CORRESPONDING VALUES

MCS	Mod.	Code Rate	n_{RB}	$\Gamma^{(LTE)}$	$\gamma_{min}^{(LTE)}$
0	QPSK	0.131	114	1.15 Mbps	-4.26
1	QPSK	0.169	88	1.49 Mbps	-3.29
2	QPSK	0.207	72	1.82 Mbps	-2.34
3	QPSK	0.266	56	2.34 Mbps	-1.18
4	QPSK	0.324	46	2.85 Mbps	-0.34
5	QPSK	0.407	38	3.59 Mbps	0.86
6	QPSK	0.484	32	4.26 Mbps	1.94
7	QPSK	0.573	26	5.05 Mbps	3.06
8	QPSK	0.645	24	5.68 Mbps	4.02
9	QPSK	0.731	22	6.44 Mbps	5.38
11	QPSK	0.804	20	7.08 Mbps	6.32
12	16QAM	0.465	16	8.20 Mbps	7.42
13	16QAM	0.532	14	9.37 Mbps	8.46
15	16QAM	0.670	12	11.80 Mbps	10.62
17	16QAM	0.744	10	13.12 Mbps	11.90
20	16QAM	1.005	8	17.71 Mbps	18.90

P_b = 200 bytes and 10 MHz bandwidth

A. Exponential Effective SNR Mapping (EESM)

EESM is derived by upper bounding the symbol error probability using Chernoff bound [9]. The generalized expression for effective SNR (γ_{eff}) using EESM is

$$\gamma_{\text{eff}} = -\beta \ln\left(\frac{1}{N}\sum_{n=1}^{N}\exp\left(-\frac{\gamma_n}{\beta}\right)\right), \quad (1)$$

where N is the number of sub-carriers and γ_n is the post-processing received SNR at the nth sub-carrier. The parameter β depends on modulation and channel conditions and optimum value of β_{opt} is the least square fit that minimizes the mean square error (MSE) between ESNR and AWGN SNR [9]. Thus, we can write

$$\beta_{\text{opt}} = \arg\min_{\beta} \left|\gamma_{\text{AWGN}} - \gamma_{\text{eff}}(\beta)\right|^2. \quad (2)$$

B. Received Bit Information Rate (RBIR)

RBIR compute effective SNR from received symbol-level mutual information [2]. The effective SNR expression in RBIR is

$$\gamma_{eff} = \beta\Phi^{-1}\left\{\frac{1}{N}\sum_{n=1}^{N}\Phi\left(\frac{\gamma_n}{\beta}\right)\right\} \quad (3)$$

where Φ is the mutual information per symbol

$$\Phi(\gamma, M) = log_2(M) - \frac{1}{M}\sum_{m=1}^{M} E_U\left\{\log_2\left(\sum_{k=1}^{M}\exp\left(|U|^2 - |\sqrt{\gamma}(s_k - s_m) + U|^2\right)\right)\right\} \quad (4)$$

where U is a zero-mean complex Gaussian random variable with unit variance and M is the modulation order.

C. Enhanced EESM (eEESM)

To obtain a more accurate link-quality metric, we presented eEESM derived from a tighter bound on SER, given by $Q(x) \leq \frac{1}{\sqrt{2\pi}x} \exp\left(-\frac{x^2}{2}\right)$ [10, eq.(11)]. Using this bound, SER for BPSK can be written as [11]

$$P_s \leq \frac{1}{\sqrt{4\pi\gamma}} \exp(-\gamma). \quad (5)$$

Consequently, for N subcarriers (5) can be expressed as

$$P_s \leq \frac{1}{\sqrt{\gamma_{\text{eff}}}} \exp(-\gamma_{\text{eff}}) = \frac{1}{N} \sum_{n=1}^{N} \frac{1}{\sqrt{\gamma_n}} \exp(-\gamma_n). \quad (6)$$

After rearranging (6), we get

$$2\gamma_{\text{eff}} \exp(2\gamma_{\text{eff}}) = 2 \left(\frac{1}{N} \sum_{n=1}^{N} \frac{1}{\sqrt{\gamma_n}} \exp(-\gamma_n) \right)^{-2}. \quad (7)$$

The generalized expression for eEESM is written as

$$\gamma_{\text{eff}} = \frac{\beta}{2} \mathcal{W} \left(\frac{2}{\beta} \left(\frac{1}{N} \sum_{n=1}^{N} \frac{1}{\sqrt{\gamma_n}} e^{-\gamma_n/\beta} \right)^{-2} \right), \quad (8)$$

where $\mathcal{W}(\cdot)$ is the Lambert-W function [12].

D. Average Effective SNR Mapping (AESM)

In order to map instantaneous SNR per sub-carriers to single effective SNR a simple approach could be to compute the average SNR. In general, for *N* sub-carriers, it can be written as

$$\gamma_{eff} = \beta \left(\frac{1}{N} \sum_{n=1}^{N} \gamma_n \right). \quad (9)$$

This approach is proposed here for SC-FDM based systems where one symbol is transmitted over all sub-carriers. It can also be used in OFDM based system as an approximation. However, it cannot provide accurate results under frequency selective fading, as shown in Section IV.

E. PHY Abstraction techniques for IEEE 802.11p

In OFDM based systems, each sub-carrier could have different probability of symbol error due to frequency selective fading. The overall SER can be expressed as

$$SER_{\text{eff}} = \frac{1}{N} \sum_{n=1}^{N} SER_n, \quad (10)$$

where SER_n is the symbol error probability at nth sub-carrier and *N* is the number of OFDM sub-carriers. In case of BPSK (10) can be expressed in term effective SNR (γ_{eff}) as

$$Q\left(\sqrt{2\gamma_{\text{eff}}}\right) = \frac{1}{N} \sum_{n=1}^{N} Q\left(\sqrt{2\gamma_{\text{n}}}\right), \quad (11)$$

TABLE III
IEEE 802.11P: PERFORMANCE COMPARISON OF PLAS

MCS	RBIR		EESM		eEESM		$\gamma_{\text{min}}^{(11p)}$
	β	MSE	β	MSE	β	MSE	
0	0.6	0.20	0.5	0.22	0.8	0.13	1.6
1	0.8	0.23	0.7	0.25	1.0	0.17	4.2
2	0.6	0.20	1.0	0.21	1.6	0.13	4.8
3	0.8	0.24	1.4	0.26	2.0	0.18	7.2
4	0.4	0.23	3.5	0.25	5.7	0.16	10.5
5	0.8	0.26	6.4	0.28	9.5	0.19	13.5
6	0.5	0.27	16	0.28	24	0.19	18.0
7	0.7	0.29	24	0.32	36	0.21	19.5

where γ_{n} is the received SNR at nth sub-carrier. Effective SNR can be calculated using EESM, eEESM and RBIR methods. However, AESM is not a good approximation compared to EESM, as $\gamma_{\text{eff}} \neq \frac{1}{N} \sum_{n=1}^{N} \gamma_{\text{n}}$.

1) Comparison with unoptimized β: Fig. 1(a) shows the PER of EESM, RBIR and eEESM, in comparison to an AWGN reference curve, without optimizing β. The relevant simulation parameters are given in Table IV. The results show that eEESM is closer to the reference curve and outperforms RBIR and EESM. In contrast, EESM and RBIR are shifted away from the AWGN curve by almost 1 and 0.6 dB respectively. This is because eEESM is derived from a tighter bound and hence is more accurate for PER prediction.

2) Comparison with optimized β: The tuning parameter β is optimized here for each MCS using (2). The optimized values of β and resulting RMSE are summarized in Table III. In Fig. 1(b) PER vs ESNR is plotted. It can be observed that β optimization significantly improves the performance. However, the MSE of eEESM is still much lower than other state of the art algorithms.

F. PHY Abstraction techniques for LTE-V2V

As explained in Section II, LTE-V2V is based on SC-FDM. In SC-FDM, an additional DFT stage is used to spread the transmitted symbols over all sub-carriers to reduce the peak-to-average power ratio (PAPR). Therefore, in frequency selective channels each symbol experiences similar channel condition. Hence, the received SNR of each symbol is the same, although the sub-carrier SNRs are different. For this reason, EESM, RBIR and eEESM, which map different symbol SNRs to a single ESNR, are not required. Therefore, instead of calculating the symbol SNR, which requires additional calculation efforts, we propose to use the average SNR over all sub-carriers as a LQM, given by AESM in (9).

1) Comparison with unoptimized β: In Fig. 2(a), ESNR vs PER is plotted for different MCS in fading channels. The relevant simulation parameters are listed in Table II and IV. The results show that the predicted PER is closer to the reference curve with a slight shift of $<$ 0.3 dB. However, the difference between the

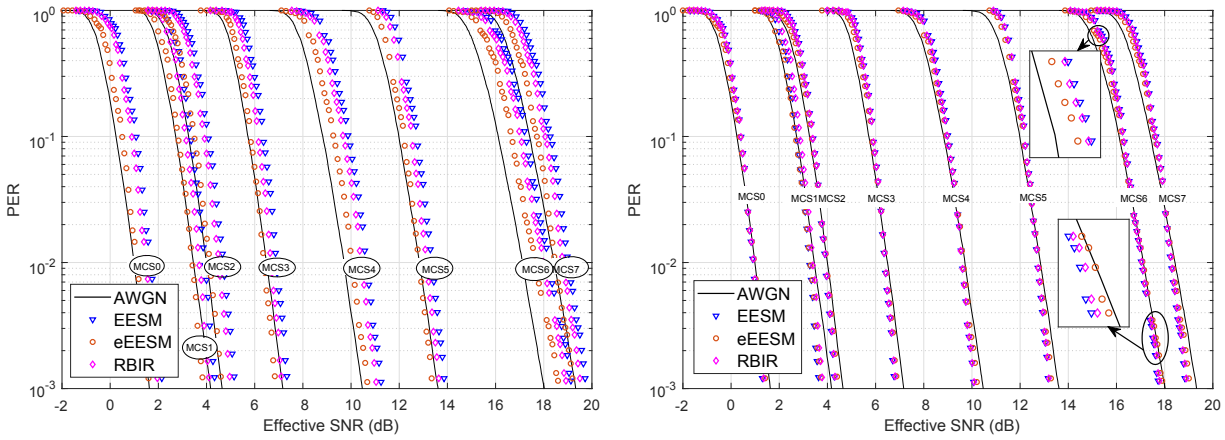

(a) PER vs ESNR

(b) PER vs ESNR with β_{opt}

Fig. 1. IEEE 802.11p: PER vs Effective SNR for various MCSs

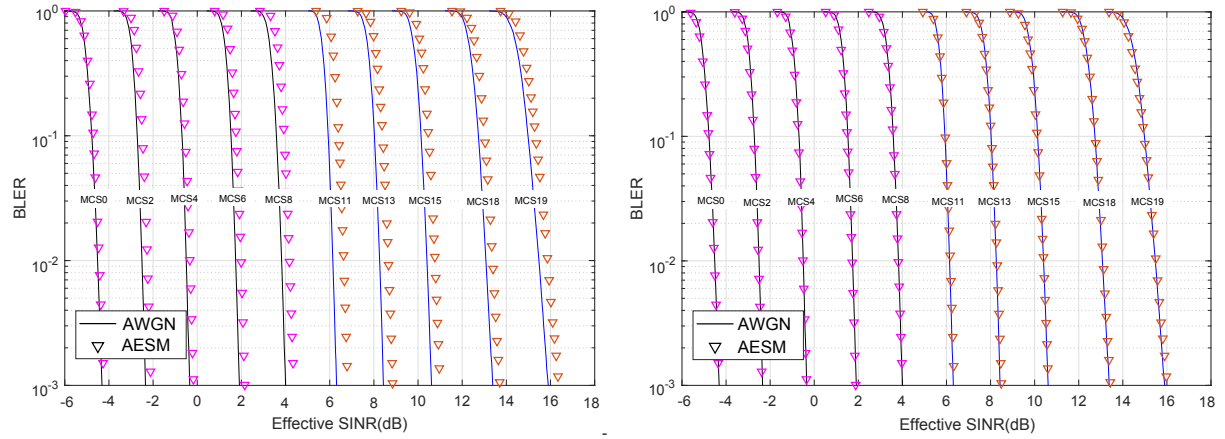

(a) PER vs ESNR

(b) PER vs ESNR with β_{opt}

Fig. 2. LTE-V2V: PER vs Effective SNR for selected MCSs

reference curve and the predicted one increases slightly with increasing modulation order.

2) Comparison with optimized β: Similar to the case of EESM, RBIR and eEESM in Section III-E, to reduce the error between reference and predicted curve, we also optimize β for AESM. In order to reduce the optimization efforts, we use a common value of β (equal to 0.9) for all MCSs because the difference between individual values of optimized β per MCS is marginal. Fig. 2(b) shows almost accurate mapping to the reference AWGN curve after optimization of β.

IV. System-Level Evaluation

In this section, technology specific system-level simulators are used to evaluate the considered PHY abstraction algorithms. The relevant simulation parameters are summarized in Table IV. To be consistent with existing literature on evaluation of V2V technologies, the path loss model and common parameters listed in Table IV are adapted from [1], [13]. The fading channel is modeled based on measurement results given in [14] for a V2V street crossing NLOS scenario at 5.9 GHz. In these simulators, one source and one destination is considered, therefore, interference is not relevant. However, in the case of multiuser scenario, SNR will be replaced by signal-to-interference ratio (SINR). To use adaptive MCS, SNR thresholds are provided in Table I & II. These values are obtained from Fig. 1 & 2 for the considered PER ($\leq 10^{-3}$).

The concept of system-level simulator is elaborated in Fig. 3. Depending on the distance and frequency response of the channel, the received SNR per sub-carrier is calculated as

$$\gamma_n = \frac{P_{\text{tx}} \cdot G_{\text{rx}}}{L_0 \cdot d^{\alpha} \cdot P_{\text{n}}} \cdot |H_n(f)|^2, \tag{12}$$

where P_{tx} is the transmit power, G_{rx} is the receive antenna gain, L_0 is the path-loss at a reference distance of 1m, d is the distance between transmitter and receiver in meters, α is the path loss exponent, P_{n} is the noise power and $H_n(f)$ is the frequency response at nth sub-carrier. The received SNR per sub-carrier is then

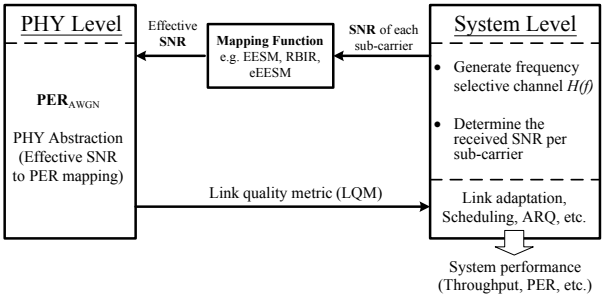

Fig. 3. PLA and its application in system-level simulations

mapped to an effective SNR, using PHY abstraction algorithms. Afterwards, a suitable MCS is selected for the next transmission from Table I or II. Furthermore, based on the selected MCS, throughput and transmission latency is estimated for respective technology by using Table I & II. The process is repeated for different channel realizations to calculate average data rates and latency. The estimated throughput using different algorithms is then compared with actual throughput (e.g obtained through PLS).

For PHY simulations, the physical layer blocks are implemented according to the respective standards. The random generated payload data is processed through transmitter chain (e.g. scrambling, encoding, interleaving, modulation, resource mapping, IFFT, adding cyclic prefix and preamble). The generated waveform is convolved with the multi-path channel impulse response. On the receiver side, preamble is used for packet detection, coarse frequency off-set correction and channel estimation. The received data is processed through receiver chain (e.g. cyclic prefix removal, FFT, resource demapping, equalization, de-modulation, de-interleaving, de-coding and de-scrambling). The recovered data is finally compared with the transmitted one and consequently, PER and throughput is calculated.

A. Performance of IEEE 802.11p based PLA

For evaluation of the abstraction techniques, an 802.11p based system-level simulator is used. Fig. 4(a) shows predicted data rates versus distance using abstraction algorithms with and without β optimization. Considering the unoptimized case, eEESM performs best and AESM worst which matches with our observations in Section III-E, whereas performance of RBIR is slightly better than EESM. Furthermore, it can be observed that the difference between predicted data rate and actual rate is almost zero, for $d \leq 10$ m and $d \geq 400$ m. The reasons behind is that either the received SNR is high enough that all algorithms select the highest MCS (in the case of $d \leq 10$ m) or the system is in outage (in the case of $d \geq 400$ m). In case of optimized β, performance of eEESM, RBIR and EESM is compared. Results show that the β optimization considerably improves the performance of all algorithms. Even though the difference in predicted data rate through different algorithms becomes marginal, eEESM still outperforms the state-of-the-art algorithms.

TABLE IV
MAIN NOTATIONS AND SETTINGS OF SIMULATION PARAMETERS

Parameter	Value
Common	
Equivalent radiated power (P_{tx})	23 dBm
Receiver antenna gain (G_{rx})	3 dB
Path loss at 1 m and at 5.9 GHz (L_0)	47.86 dB
Loss exponent (α)	2.75
Distance (d)	Variable input
Noise power over 10 MHz (P_n)	-95 dB
Payload size (P_b)	200 bytes
Specific for IEEE 802.11p	
Carrier Spacing	156.25 KHz
Symbol duration	6.4 μs
Cyclic prefix	1.6 μs
Number of useful sub-carriers	52
Minimum SNR for target PER ($\gamma_{min}^{(11p)}$)	From Fig. 1
Transmission latency ($t_{\text{tx}}^{(11p)}$)	Given in Table I
Data rate ($\Gamma^{(11p)}$)	Given in Table I
Specific for LTE-V2V	
Carrier Spacing	15 KHz
Symbol duration	66.7 μs
Cyclic prefix (1^{st} /following symbols)	5.2 / 4.69 μs
Number of resource blocks (n_{RB})	Given in Table II
Minimum SNR for target PER ($\gamma_{min}^{(\text{LTE})}$)	From Fig. 2
Transmission latency ($t_{\text{tx}}^{(\text{LTE})}$)	2 /1 ms (MCS0 /else)
Data rate ($\Gamma^{(\text{LTE})}$)	Given in Table II
Channel specific parameters	
Maximum differential speed	126 km/hr
RMS delay spread	200 ns
Coherence bandwidth (50%)	$\approx$1 MHz
Relative power of each tap	[0 -3 -5 -10] dB
Excess delay of each tap	[0 267 400 533] ns
Doppler spread of each tap	[0 295 -98 591] Hz

B. Performance of LTE-V2V based PLA

Similar to the case of 802.11p, a LTE-V2V system-level simulator is used to evaluate performance of the proposed AESM algorithm. The hybrid automated repeat request (HARQ) process is not modeled since single shot communication is considered due to low latency requirements. In Fig. 4(b), the predicted data rate versus distance is plotted for AESM with and without optimization of β. For the unoptimized case, it is observed from results that AESM is considerably accurate in predicting the data rate for $d \geq 150$ m. The reason is, for lower values of effective SNR (< 11.9 dB), the step sizes for choosing different MCSs are smaller and differences in resulting data rates are also smaller, which is mostly the case for higher values of d. However, for effective SNR ≥ 11.9 dB the next suitable MCS is at 18.90 dB (a difference of 7 dB) and resulting data rate difference is 4 Mbps. This results in a higher error if the selected MCS based on AESM differs from the actual MCS (chosen by PLS), which is due to the small packet size required for most V2X applications [15]. In the case of

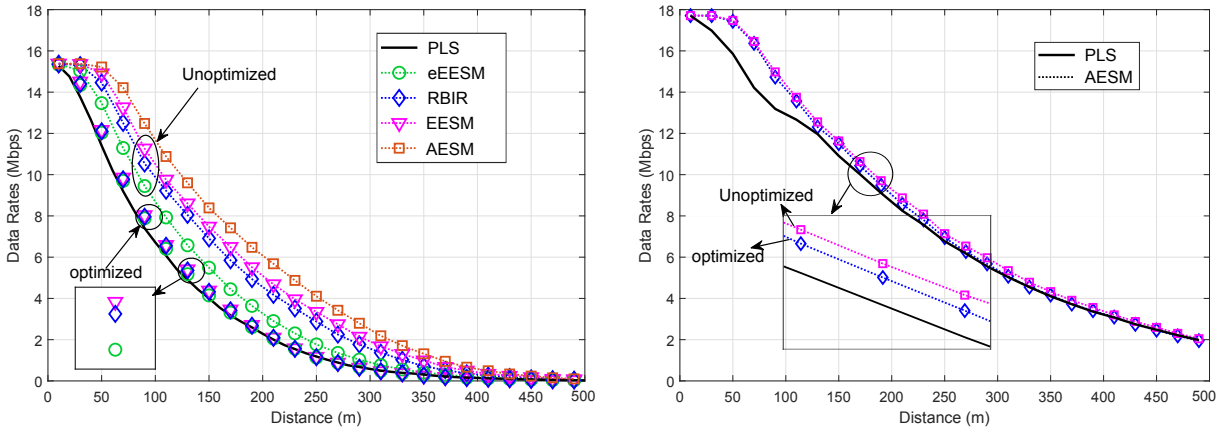

(a) IEEE 802.11p

(b) LTE-V2V

Fig. 4. Performance comparison of PLAs in system-level simulation

optimized β, the performance is slightly better compared to the unoptimized case for d $\geq$ 100 m. As the received SNR of each sub-carrier has no direct mapping to SER the performance of AESM is less sensitive to channel variations.

V. Comparison of Technologies

In order to highlight applications of PLA, we provide a comparison between 802.11p with eEESM and LTE-V2V with AESM in terms of data rate, transmission latency and packet reception ratio (PRR). Based on the channel conditions and distance, effective SNR is computed, which is further mapped to an MCS. The minimum SNR required for each MCS, which fulfills a certain reliability constraint, can be obtained from Fig. 1 & 2. Based on the selected MCS, data rates and transmission latencies are obtained from Table I & II. The procedure is repeated for multiple channel realizations to obtain mean values.

Fig. 5(a) shows the average data rates versus the distance for various reliability requirements. In terms of data rates and coverage LTE-V2V is superior than 802.11p due to the following reasons: First, it uses turbo coding, which has better error correction capabilities compared to convolution coding used in 802.11p. Second, SC-FDM has higher transmission efficiency due to lower PAPR (peak-to-average-power-ratio). Third, longer transmission time in LTE-V2V leads to higher energy per bit. In addition, 802.11p uses a fixed preamble of 40 μs, which is a significant overhead for short package transmission, as in the case of V2X applications [15]. However in case of LTE-V2V, the equivalent data rates given in Table II are independent of payload size, due to transmission of control information on separate control channels. Another observation from Fig. 5(a), is that LTE-V2V data rates are less sensitive to different PER requirements. This is due to sharp decrease in PER by increasing SNR in case of turbo coding (as seen in Fig 2(a)). Furthermore, LTE-V2V uses a large set of MCS, allowing fine-grained link adaptation. In contrast, 802.11p data rates drops considerably with increasing reliability.

The transmission latency versus distance is plotted in Fig. 5(b) for various PER constraints. Results show that 802.11p has much lower latency compared to LTE-V2V, which is due to the fact that in 802.11p transmission time is defined by the payload size and the selected MCS. Either increasing distance or guaranteeing higher reliability lead to a larger transmission latency due to usage of lower MCSs. On the other hand, transmission latency for LTE-V2V is almost constant for d $<$ 250 m and increases with distances higher than 250 m due to the use of MCS0. Similar to the case of data rates, transmission latency of LTE-V2V is less sensitive to different PER constraints because transmission latency does not vary with MCS selection except in the case of MCS0.

In Fig. 5(c), the performance of both technologies is compared in term of PRR (packet reception ratio). For calculating PRR of a given MCS at a certain distance, the effective SNR is mapped to a PRR by using precomputed (through AWGN simulation) ESNR vs PRR lookup tables. Three different MCSs from each technology are selected for comparison. First, the lowest possible MCS of each technology (MCS0) is evaluated, which defines the maximum range of a technology. For example, considering PRR $>$ 90%, LTE coverage is around 410 m, which is more than twice the range of 802.11p ($\approx$ 180 m). The reason for that is the minimum code rates of 0.1 used in LTE against 0.5 in 802.11p. Therefore for a fair comparison, MCS2 (1/2 QPSK) & MCS4 (1/2 16QAM) of 802.11p are compared against MCS6 ($\approx$ 1/2 QPSK) & MCS13 ($\approx$ 1/2 16QAM) of LTE. As a result, using same code rate and modulation scheme, LTE can still achieve higher range (double)

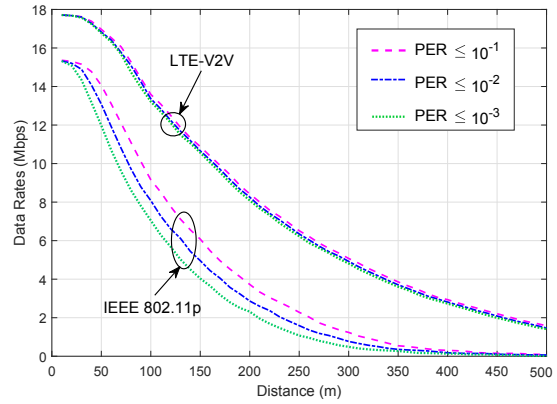

(a) Throughput vs distance

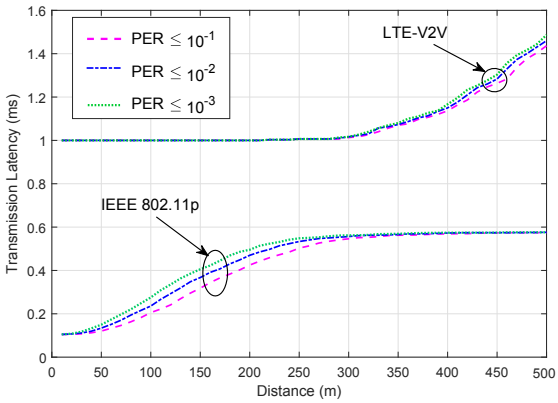

(b) Latency vs distance

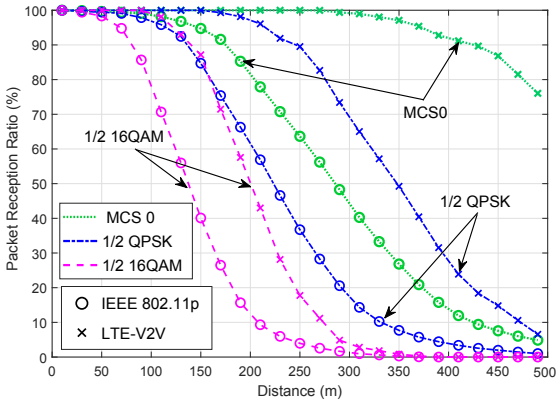

(c) Packet reception ratio (%) vs distance

Fig. 5. Performance comparison between IEEE 802.11p and LTE-V2V

than 802.11p. The reasons are again more sophisticated channel coding, the DFT-spread of the symbols and a higher energy per bit.

VI. Conclusions

In this paper, we presented different PLA techniques for IEEE 802.11p and LTE-V2V, and compared their performance in technology specific system-level simulations. The results show that the proposed algorithms, enhanced EESM for 802.11p and AESM for LTE-V2V can accurately predict the throughput, latency and PER performance. Moreover, eEESM outperforms state-of-the-art algorithms such as EESM and RBIR. In addition, comparison between both technologies is provided in terms of throughput, latency and packet reception ratio for fading channels. It is observed that LTE-V2V performs better than 802.11p in terms of average data rates, packet reception ratio and coverage. This is due to advanced channel coding, DFT-Spread of symbols and longer transmission time. In contrast, 802.11p is better in terms of transmission latency due to the shorter transmission time.

Acknowledgment

This work is supported by the Federal Ministry of Education and Research of the Federal Republic of Germany (BMBF) in the framework of the project 5G NetMobil with funding number 16KIS0688. The authors alone are responsible for the content of the paper.

References

[1] A. Bazzi, B. Masini, A. Zanella, and I. Thibault, "On the performance of IEEE 802.11p and LTE-V2V for the cooperative awareness of connected vehicles," pp. 1–1, 09 2017.

[2] R. Hoefel and O. Bejarano, "On application of phy layer abstraction techniques for system level simulation and adaptive modulation in IEEE 802.11ac/ax systems," vol. 31, 01 2016.

[3] J. Wu, Z. Yin, J. Zhang, and W. Heng, "Physical layer abstraction algorithms research for 802.11n and lte downlink," in *International Symposium on Signals, Systems and Electronics*, 2010.

[4] "IEEE standard for information technology - specific requirements - part 11: Wireless LAN medium access control (MAC) and physical layer (PHY) specifications," *IEEE Std 802.11-2016*.

[5] X. Huang, D. Zhao, and H. Peng, "Empirical study of DSRC performance based on safety pilot model deployment data," *IEEE Transactions on Intelligent Transportation Systems*, vol. 18, no. 10, 2017.

[6] S. E. Carpenter and M. L. Sichitiu, "Analysis of packet loss in a large-scale DSRC field operational test," in *2016 International Conference on Performance Evaluation and Modeling in Wired and Wireless Networks (PEMWN)*, Nov 2016, pp. 1–6.

[7] 3GPP: Initial Cellular V2X standard completed, sep. 2017. [Online]. Available: http://www.3gpp.org/release-14

[8] Technical Specification Group Radio Access Networks, "Evolved universal terrestrial radio access (E-UTRA); physical layer procedures," *3GPP TS 36.213 V14.3.0*, Jun. 2017.

[9] J. Olmos, A. Serra, S. Ruiz, M. Garca-Lozano, and D. Gonzalez, "Exponential effective sir metric for lte downlink," in *2009 IEEE 20th International Symposium on Personal, Indoor and Mobile Radio Communications*, Sept 2009, pp. 900–904.

[10] S. A. Dyer and J. S. Dyer, "Approximations to error functions," *IEEE Instrumentation Measurement Magazine*, vol. 10, no. 6, pp. 45–48, December 2007.

[11] J. R. Barry, D. G. Messerschmitt, and E. A. Lee, *Digital Communication: Third Edition*. Norwell, MA, USA: Kluwer Academic Publishers, 2003.

[12] R. M. Corless, G. H. Gonnet, D. E. G. Hare, D. J. Jeffrey, and D. E. Knuth, "On the LambertW function," *Advances in Computational Mathematics*, vol. 5, no. 1, Dec 1996.

[13] A. Bazzi, B. M. Masini, A. Zanella, and I. Thibault, "Beaconing from connected vehicles: IEEE 802.11p vs. LTE-V2V," in *27th Annual International Symposium on Personal, Indoor, and Mobile Radio Communications (PIMRC)*, 2016.

[14] M. Kahn, "V2V radio channel models," *IEEE 802.11-14/0259r0*, Feb. 2014.

[15] 5G Alliance for Connected Industries and Automation, "5G for connected industries and automation (white paper)," April 2018.